

AD-A166 747

CHINESE JOURNAL OF LASERS THE TENTH YEAR (1974-1984)

1/1

(SELECTED ARTICLES)(U) FOREIGN TECHNOLOGY DIV

WRIGHT-PATTERSON AFB OH 2 MEIZHEN ET AL. 11 APR 86

UNCLASSIFIED

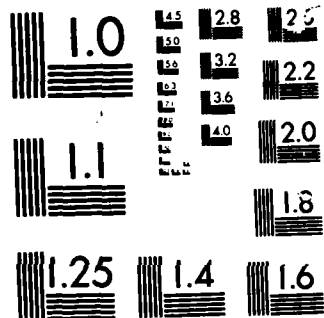
FTD-ID(RS)T-0006-86

F/G 20/5

NL

		0											

END



MICROCOPY

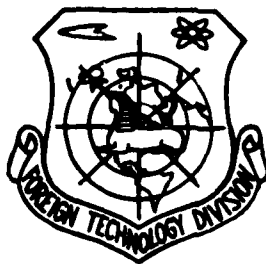
CHART

2  
FTD-ID(RS)T-0006-86

# FOREIGN TECHNOLOGY DIVISION



CHINESE JOURNAL OF LASERS  
THE TENTH YEAR  
(1974-1984)  
(Selected Articles)



DTIC  
ELECTE  
APR 22 1986  
S A

Approved for public release;  
Distribution unlimited.

AD-A166 747

DTIC FILE COPY

86 4 21 033

## HUMAN TRANSLATION

FTD-ID(RS)T-0006-86

11 April 1986

MICROFICHE NR: FTD-86-C-001713

CHINESE JOURNAL OF LASERS. THE TENTH YEAR (1974-1984)  
(Selected Articles)

English pages: 22

Source: Zhong Guo Jiguang, Vol. 11, Nr. 11, 1984,  
pp. 665-666; 686-690

Country of origin: China

Translated by: SCITRAN

F33657-84-D-0165

Requester: FTD/SDEO

Approved for public release; distribution unlimited.

THIS TRANSLATION IS A RENDITION OF THE ORIGINAL FOREIGN TEXT WITHOUT ANY ANALYTICAL OR EDITORIAL COMMENT. STATEMENTS OR THEORIES ADVOCATED OR IMPLIED ARE THOSE OF THE SOURCE AND DO NOT NECESSARILY REFLECT THE POSITION OR OPINION OF THE FOREIGN TECHNOLOGY DIVISION.

PREPARED BY:

TRANSLATION DIVISION  
FOREIGN TECHNOLOGY DIVISION  
WPAFB, OHIO



GRAPHICS DISCLAIMER

All figures, graphics, tables, equations, etc.  
merged into this translation were extracted  
from the best quality copy available.

↙  
Lasing Characteristics of High Quality Nd:YAG  
Crystals Grown by Temperature Gradient Technique,

Zhang Meizhen, Li Chengfu, Zhou Yongzong

Shanghai Institute of Optical and Fine Mechanics  
Chinese Academy of Sciences

ABSTRACT

↘ A Nd:YAG crystal of  $\phi 5 \times 50$  mm in size was grown by a temperature gradient technique. It has good optical homogeneity (interference fringe number is zero) and an efficiency of 1 % at 1 or 2 pps. It is easy to be operated in TEM<sub>00</sub> mode. 7

1. INTRODUCTION

Until now Nd:YAG crystal is still the laser material with the best quality and is most widely used in the field of laser applications. Until now the production method is mainly the upward guiding method. But this method has certain limitation for obtaining large diameter crystal material with good optical uniformity in a large area. Therefore a new processing method must be sought. It was known that the United States recently had grown good optical quality crystals with a size of  $\phi 100 \times 100$  mm by heat exchange (

i.e. temperature gradient) method. With this new method, our country has obtained  $\phi 50 \times 62$  mm Nd:YAG crystal with 0.9-1.3 % Nd doping concentration. Such crystal has good optical uniformity, less scattering centers, low dislocations. In order to study the lasing characteristics of crystal prepared by such method, we processed the crystal into a  $\phi 5 \times 50$  rod (interference fringe is zero, see Fig. 1.) and made systematic measurements of its lasing characteristics with repeating frequency laser devices. The experimental results show the average efficiency is close to 1 % and the maximum power output can reach 3.0 million watts (pulse width is 10 ns). Because the optical uniformity of the sample rod is very good, it is easy to obtain a stable output of single transverse mode.



Fig. 1. The Tyman-Green interference pattern of the crystal rod (by courtesy of Gu Yazhen)

---

Received by Oct. 31, 1983.

## 2. EXPERIMENTAL METHOD AND RESULTS

The experimental arrangement is shown in Fig. 2. The laser device is a plano-concave type stable cavity. The rear reflection cavity plate is a  $1.06 \mu\text{m}$  total reflection concave lens with  $R = 3 \text{ m}$ . The front cavity plate is a  $1.06 \mu\text{m}$  flat plate with a 40 % transparency. The cavity length is 480 mm. A LiF crystal irradiated by a  $\text{Co}^{60}$  radiation source is used as Q adjustment switch. With single lamp pumping, the repeating rates of the device are 0.5, 1, 2, and  $5 \text{ sec}^{-1}$ . The diameter of grating used for mode selection is  $\phi 0.81 \text{ mm}$ . The pulse width of the laser after the Q adjustment is 10 ns.



Fig. 2. The arrangement of the laser device

- (1) The distribution of the laser beam spot
- (a) Static status (without Q adjustment): The patterns near the field and 1 meter from the cavity plate were

obtained by using photographic black paper. The result shows the field of the output laser beam is quite uniform.

(b) Field distribution of single transverse mode output (with Q adjustment): The single transverse mode was selected by use of a  $\phi 0.81$  mm small hole. Near the threshold (input energy was 0.37 Joule), we found a stable  $TEM_{00}$  output can be easily obtained by such crystal rod. The field distribution of 8 meters from the cavity plate was photographed (Fig. 3a.). Fig. 3b. shows the result by the scanning of a blackness meter. In Fig. 3b, the solid line is the experimentally measured result, and the dashed line is the calculated curve of Gaussian distribution function

$$I = I_0 e^{-r^2/a^2}$$

From this figure we can know that the experimental results fit very well with the theoretical values and this is a proof of the single transverse mode.

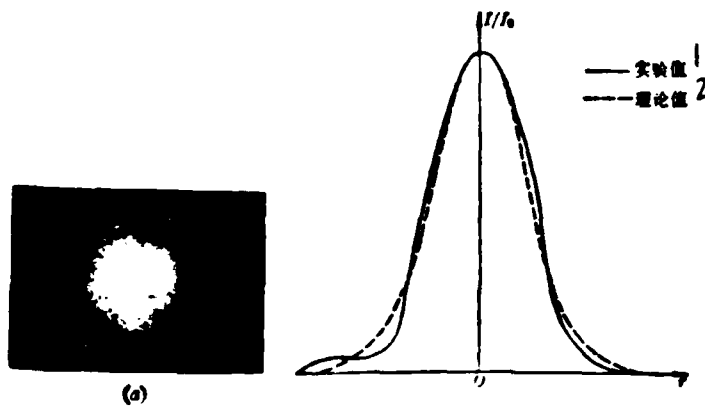


Fig. 3. The field distribution of the laser single transverse mode. 1 - experimental results; 2 - theoretical results;

(2) Energy output

(a) Static output efficiency (without Q adjustment, the pulse width was 100 ns): The experimental results are listed in table 1. From table 1, we know that the average efficiency can reach about 1 %.

(b) Dynamic power output: The laser power output was measured during the Q adjustment (the pulse width of device was 10 ns). The experimental result is listed in table 2. The experimental result shows that under our device conditions, the output power can reach above 3 million watts.

Table 1. Static efficiency  
(input capacitance is 100 uf)

1 重复率 (次/秒)	2 充电电压 (伏)	3 输入能量 $E_{in}$ (焦耳)	4 输出能量 $E_{out}$ (焦耳)	5 效率 $\eta$ (%)
0.5	800	19.2	0.137	0.7
	850	22.2	0.218	1.0
	960	27.6	0.278	1.0
	1000	30.0	0.319	1.0
	1150	40.2	0.415	1.0
1.0	1160	40.2	0.449	1.1
2.0	1160	40.2	0.51	1.1

1-repeating rate ( $\text{sec}^{-1}$ ); 2-charging voltage (volt); 3-input energy (joule); 4-energy output (joule); 5-efficiency (%).

Table 2. Dynamic laser power ( $\tau=10$  ns)

重复率 (次/秒)	充电电压 (伏)	输入能量 $E_{in}$ (焦耳)	输出能量 $E_{out}$ (毫焦耳)	输出功率 $W_{out}$ (兆瓦)
0.5	960	27.6	29.0	2.9
	1000	30.0	29.1	2.9
	1160	40.0	30.2	3.0
1.0	1160	40.0	32.4	3.24

1-repeating rate ( $\text{sec}^{-1}$ ); 2-charging voltage; 3-input energy (joule); 4-energy output (joule); 5-power output (millin watts).

(c) The laser energy of the single transverse mode: the output energy in  $\text{TEM}_{00}$  mode (with Q adjustment) is 2.8 milli-joules when the energy input is 37 joules.

#### REFERENCE

[1] Zhou Yongzong, et al, Journal of Silicates ( a magazine published by the Chinese Academy of Sciences), No. 11, 1983, pp. 357-360.

# Antireflective Coating with High Efficiency at 1.06 $\mu\text{m}$

Fan Relying, Lu Yuemei

Shanghai Institute of Optics and Fine Mechanics,  
Chinese Academy of Science

## ABSTRACT

The error of the two-layer antireflective coating is analysed. It is shown that optical properties of the film composed of non-quarter wavelength stack is more stable than those of the film composed of quarter wavelength stack. The two-layer antireflective film has been made on  $\text{K}_9$  substrate and  $\text{Ta}_2\text{O}_5$  and  $\text{SiO}_2$  used as coating material. Its reflectivity at one surface is lower than 0.03% and laser induced damage threshold is over 7  $\text{GW}/\text{cm}^2$  (at 1.06  $\mu\text{m}$  and 1 ns).

## 1. INTRODUCTION

In laser systems, the aperture expansion telescope in a laser multi-amplification system and all other lenses require antireflective film coating. Low reflection, on the one hand, enables the great increase of laser output, and on the other hand, prevents the damage of optical elements by

the reflected light from the lens surfaces.

Limited by the film material itself, the antireflection effect of a single layer film could not be very high, and it can not meet the requirement of high power laser systems. Therefore double- or multi-layer antireflection systems have to be used. Because only single wavelength antireflection is required and also because of simplicity and the possibility of processing are considered, a double-layer antireflection system was chosen. In order to obtain a good processing reproducibility, we have made error analysis on quarter and non-quarter double-layer wavelength films, and the non-quarter double-layer system, which has a wider allowed error of optical thickness, was chosen as a better antireflective system. We also made experimental studies on the coating materials, found the processing conditions for obtaining high efficiency antireflection, and therefore the product reproducibility can be guaranteed.

## 2. THE SELECTION OF FILM SYSTEM AND ERROR ANALYSIS

When light incidents on a transparent substrate with double-layer film coating (as shown in Fig. 1.), the reflection  $R$  is decided by the following formulas:

$$R = \frac{\{r_1^2 + r_2^2 + r_3^2 + r_1^2 r_2^2 + 2r_1 r_2 (1 + r_3^2) \cos 2\phi - 2r_2 r_3 (1 + r_1^2) \cos 2\psi\} + 2r_1 r_3 \cos 2(\phi + \psi) + 2r_1 r_2 r_3 \cos 2(\phi - \psi)}{\{1 + r_1^2 r_2^2 + r_1^2 r_3^2 + r_2^2 r_3^2 - 2r_1 r_2 (1 - r_3^2) \cos 2\phi + 2r_2 r_3 (1 + r_1^2) \cos 2\psi\} + 2r_1 r_3 \cos 2(\phi + \psi) + 2r_1 r_2 r_3 \cos 2(\phi - \psi)}$$

here  $r_1, r_2, r_3$  are Fresnel coefficients:

$$r_1 = \frac{n_0 - n_1}{n_0 + n_1}, \quad r_2 = \frac{n_1 - n_2}{n_1 + n_2},$$

$$r_3 = \frac{n_2 - n_3}{n_2 + n_3},$$

and  $\phi$  and  $\psi$  are the phase differences,

$$\phi = \frac{2\pi n_1 d_1}{\lambda}, \quad \psi = \frac{2\pi n_2 d_2}{\lambda}.$$

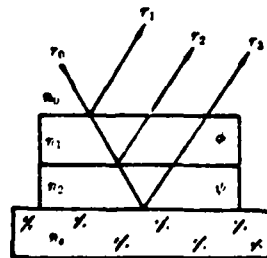


Fig. 1. Model of double-layer film

When the refractivities of coating materials are determined, zero reflection of the film system can be obtained by adjusting the thicknesses of the two film layers, that is: adjusting  $\phi$  and  $\psi$ . Generally, in the coating processing, a high reflection material with refractivity  $n_2$  is applied to the inner layer which is close to the substrate until a reflectivity  $R_m$  is obtained and the phase thickness is  $\psi$ , then a low refractivity material ( $n_1$ ) is applied for the second layer coating until a maximum value is obtained. Then the coating is continued until the second maximum value is obtained. At this stage the phase thickness of the low refractivity layer is  $\phi$ . Because the film at the stage of the first maximum value consists of two materials, the refractivity of this layer is equal to an effective refractivity  $n_e$  (as shown in Fig. 2). For simplicity we define this layer as effective layer.

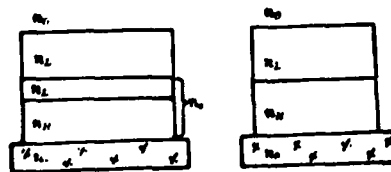


Fig. 2. quarter and non-quarter wavelength double-layer films

According to the calculation formulas we can obtain: when  $n_0=1$ ,  $n_S=1.506$ ,  $n_L=1.45$  and  $n_H=2.04$ , zero reflection at the center wavelength can be obtained if  $R_m=10.7\%$  and at this time  $n_e=1.782$ . The same result can also be obtained by the use of non-quarter film with  $n_L=1.45$  and  $n_H=n_e=1.782$ . Following is a comparative error-analysis of these two film systems:

First consider the situation when the refractivities of the coating materials deviate from the matching values in these two film systems. When they have same relative errors, their influences on the total reflection spectra are shown in table 1 and 2.

Table 1. The error of  $n_H$  is  $\pm 7.85\%$  and  $n_L=1.45$  is kept unchanged

非λ/4双单层 1			λ/4双单层 2		
$n_H$	$R_T$	$Q_{min}$	$n_e$	$R_T$	$Q_{min}$
2.04	0	1.0	1.782	0	1.0
2.20	0.0069	1.0	1.922	0.5700	1.0
1.88	0.0069	1.0	1.642	0.6600	1.0

1-non-quarter wavelength double-layer film; 2-quarter wavelength double-layer film

Table 2. The error of  $n_L$  is  $\pm 6.9\%$  and  $n_H=2.04$  and  $n_e=1.782$  are kept unchanged

非λ/4双层层膜 1			λ/4双层层膜 2		
$n_L$	$R_{\min}$	$g_{\min}$	$n_L$	$R_{\min}$	$g_{\min}$
1.45	0	1.0	1.45	0	1.0
1.55	0.25%	1.01	1.55	0.44%	1.0
1.35	0.33%	0.985	1.35	0.51%	1.0

1-non-quarter wavelength double-layer film; 2-quarter wavelength double-layer film; 3-note:  $g_{\min}(=\lambda_0/\lambda_{\min})$  is the relative wave number when the reflection is minimum.

From table 1 and 2 we can know: when the refractivities of the film materials deviate from the matching values, their influences to the minimum values of the deflectivity in non-quarter wavelength double-layer film is less than in the quarter wavelength double-layer film, and this is especially obvious by the error of the high refractivity materials.

Furthermore, if we analyze the influence of the controlled errors of these two film systems on the total optical spectral characteristics of the reflection (when the refractivities are kept unchanged, it will reflect the errors of the layer thickness), we found that the influence of the layer thickness is negligible comparing with the

influences by the errors of the reflectivities.

The total errors are mainly introduced by the refractivities of the coating materials (table 3 lists the situation, for non-quarter wavelength, when the inner and outer layers have the same controlled error), for the non-quarter double-layer film. Therefore it is determined that the non-quarter wavelength double-layer film system is more stable than the quarter wavelength double-layer film system. Furthermore it is also less influenced by the refractivities of film materials. Thus we chose it as our experimental film system. The specific system is as follows: A( $\alpha_1$ L,  $\alpha_2$ H)G( $\alpha_1$ ,  $\alpha_2$  are the relative thicknesses to  $\lambda/4$ ,  $\alpha_2 < 1$ ,  $\alpha_1 > 1$ ), the relative phase thicknesses of the two layers are:  $\delta_L = 1.9967$  (radian) and  $\delta_H = 0.6059$  (radian), for  $n_0 = 1.0$ ,  $n_S = 1.506$ ,  $n_L = 1.45$ , and  $n_H = 2.04$ . Their optical spectrum curves are shown in Fig. 3 and  $R_{\min} = 0$  at the center wavelength.

Table. 3. The influence of the controlled errors of refractivities of the non-quarter double-layer film system

内层膜 1			外层膜 2		
$\left(\frac{\Delta R}{R}\right)_q$	$R_{\min}$	$g_{\min}$	$\left(\frac{\Delta R}{R}\right)_L$	$R_{\min}$	$g_{\min}$
$\frac{1}{100}$	0.00001%	1.0	$\frac{1}{100}$	0.005%	0.975
$\frac{1}{110}$	0.00007%	1.0	$\frac{1}{11}$	0.008%	0.965
$\frac{1}{55}$	0.00029%	1.0	$\frac{1}{55}$	0.019%	0.940

1-inner film layer; 2-outer film layer

According to table 1-3, we can know that for the non-quarter wavelength double layer system either the error of refractivity or the error of the layer thickness has a larger influence on the outer layer than on the inner layer. Therefore it is important to control rigorously the processing of the outer layer of the non-quarter double-layer film system.

### 3. PROCESSING

(1) A study of film materials

(a) Characteristics of  $Ta_2O_5$  film material

We used 99.95 % purity white  $Ta_2O_5$  powder to prepare

blocks by pressure. Such blocks were put into an oven at 900 °C for 8 hours. Then the refractivity and dispersion were studied by the E-type gun evaporation technique. Table 4-7 lists the changes of refractivity and dispersion with the changes of the processing parameters.

Table 4. The changes of n as a function of substrate temperature

t(°C)	250	280	330
n	2.067	2.077	2.083

The data in table 4 were obtained under an oxygen pressure  $2 \times 10^{-4}$  torr and the deposition velocity was 7-8 Å/sec.

Table 5. The changes of n as a function of oxygen pressure

P(O <sub>2</sub> )	$2 \times 10^{-4}$	$3 \times 10^{-4}$	$4 \times 10^{-4}$
n	2.071	2.058	2.048

1-torr.

The data in table 5 were obtained when the substrate temperature was 280 °C, deposition rate was 7-8 Å/sec, and the initial pressure was  $1 \times 10^{-4}$  torr.

Table 6 The changes of n as a function of the deposition rate

$v(\text{Å}/\text{sec})$	4~5	9
n	2.060	2.065

1-sec.

The data in table 6 were obtained when the substrate temperature was 280 °C and the pressure was  $3 \times 10^{-4}$  torr.

The above data are the average values of several experiments. n values are related to  $\lambda = 6328 \text{ Å}$  and were obtained by a TP-77 elliptical polarization thickness meter.

Table 7. The dispersion of the refractivities of  $\text{Ta}_2\text{O}_5$

$\lambda$ (微米)	1.05	0.94	0.82	0.75	0.65	0.54	0.45
n	2.05	2.053	2.056	2.061	2.066	2.072	2.11

1- $\mu\text{m}$ .

The data of table 7 were obtained under the same substrate temperature ( $300^{\circ}\text{C}$ ), the same oxygen pressure ( $1.6 \times 10^{-4}$ ) and the same deposition rate ( $8 \text{ \AA}/\text{sec}$ ).

According to the above experimental results, we know that the changes of refractivity of  $\text{Ta}_2\text{O}_5$  material is not large within certain ranges of temperature, oxygen pressure, and film deposition rate.

The results of the scattering coefficient, around  $6500 \text{ \AA}$ , of single-layer  $\text{Ta}_2\text{O}_5$  on the  $\text{K}_9$  substrate show that the scattering loss is equal to  $\text{ZrO}_2$ , but the absorbing loss is very small.

Through the experiment, it was found that under the same deposition conditions, the absorption coefficient of the film using fresh  $\text{Ta}_2\text{O}_5$  is different from the films using  $\text{Ta}_2\text{O}_5$  material which has been used for several times. The absorption coefficient of the latter is obviously larger. The cause for this is mainly because the decomposition of  $\text{Ta}_2\text{O}_5$  in the deposition process, the outgoing ratio of oxygen gas and Ta molecules is different and thus the content of the remaining  $\text{Ta}_2\text{O}_5$  undergoes some changes. Therefore after each deposition, some fresh material should be added or the oxygen gas amount should be increased to make compensation.

#### (b) Characteristics of $\text{SiO}_2$ film material

Many experimental works have already proved that the reproducibility of refractivity of  $\text{SiO}_2$  is better in an air

environment. But is it still true in the vacuum environment? Therefore systematic experiments were carried out. The quarter double-layer films prepared under different processing parameters ( $\lambda=6328 \text{ \AA}$ ) were studied and the changes before and after heat treatment (the baking temperature was  $280 \text{ }^\circ\text{C}$ ), under air and vacuum environments were studied. The obtained data are listed in table 8-10.

Table 8. The relation between  $n$  and vacuum degree

气压 $P$ (托)	$3 \times 10^{-4}$	$2 \times 10^{-4}$	$6 \sim 4 \times 10^{-5}$
$n$	1.359	1.372	1.40

1-pressure (torr).

The data in table 8 were obtained when the substrate was not heated, and the deposition rate was  $45 \text{ \AA}/\text{sec}$ .

Table 9. The relation of  $n$  and the substrate temperature

环境气氛		$T(^\circ\text{C})$		
		室温 $30^\circ\text{C}$	$25^\circ\text{C}$	$275^\circ\text{C}$
真空 $2 \times 10^{-4}$ 托		1.372	1.389	1.408
大气中	5 烘烤前	1.453	1.455	1.462
	6 烘烤后	1.447	1.448	1.446

1. atmosphere environment; 2-room temperature; 3-vacuum ( $2 \times 10^{-4}$  torr); 4-atmosphere; 5-before baking; 6-after baking.

The data in table 9 were obtained with samples prepared under a vacuum of  $2 \times 10^{-4}$  torr and a deposition rate of about  $45 \text{ \AA}/\text{sec}$ .

Table 10. The relation between  $n$  and deposition rate  $v$

环境气氛 <sup>1</sup>		$v(\text{Å}/\text{sec})^2$		
		16	45	72
		$n$		
3	真空( $2 \times 10^{-4}$ 托)	1.355	1.372	1.392
4	大气中			
	5 烘烤前	1.445	1.453	1.457
	6 烘烤后	1.441	1.447	1.447

1-atmosphere environment; 2-sec; 3-vacuum ( $10^{-4}$  torr); 4-atmosphere; 5-before baking; 6-after baking.

The data in table 10 were obtained with the samples prepared with the substrate unheated and in a vacuum of  $2 \times 10^{-4}$  torr.

From table 8-10 we can know that: (1) the refractivity of  $\text{SiO}_2$  increases with the increase of substrate temperature, vacuum degree, and deposition rate; (2) the dependence of change of refractivity of  $\text{SiO}_2$  on the deposition conditions is more sensitive in a vacuum than in atmosphere; (3) there is a reversible process of the

refractivity of  $\text{SiO}_2$  from vacuum to atmosphere and then being baked. That is: the reflectivity is lower in a vacuum, and it will increase if being put in the atmosphere, and it will decrease slightly again after being baked.

(2) Some important points for the film preparation

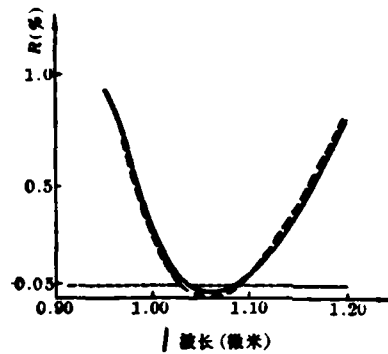
There was no special processing technique used in our antireflection coating. In order to obtain a good product reproducibility, attention should be paid to the control of processing conditions, such as the substrate temperature, oxygen pressure, deposition rate, etc. (it is especially important for  $\text{SiO}_2$  films in a vacuum, because its refractivity in a vacuum is quite sensitive and its change has a larger influence to the antireflection films). Only in this way a stable refractivity can be obtained. At the same time, attention should be paid to the difference of the refractivities of film materials in a vacuum and atmosphere. Only when the vacuum  $\delta'_H$  (it is less than the calculated  $\delta_H$  value) is obtained, can the antireflection film which has the required optical spectra characteristics be prepared.

#### 4. EXPERIMENTAL RESULTS

(1) The optical characteristics

The experimental results of the prepared samples with

the point measurements of the low reflectivity meter and with the scanning of a UV-360 spectrometer are listed in table 11 and Fig. 3. The results show the single surface reflectivity of the  $K_g$  substrate;  $R$  is less than 0.03 % around the wavelength of  $1.06 \mu\text{m}$ .



2 图3 实验结果与理论计算比较

3 — 实验曲线 4 — 理论曲线

Fig. 3. A comparison of the experimental results and theoretical calculation

1-wavelength; 2-caption; 3-measured curve; 4-theoretical curve.

The scattering coefficient measured with a scattering apparatus is  $1-1.5 \times 10^{-4}$  for  $\lambda = 0.65 \mu\text{m}$  and it is a little lower than the scattering by the  $\text{Ta}_2\text{O}_5$  film.

(2) The damage threshold by laser

the damage threshold of this antireflection film is about 7-8 billion watts/cm<sup>2</sup> measured with a  $1.06 \mu\text{m}$  laser beam of 1 ns pulse width. This can meet the requirement by

high power laser systems.

样 品 号	$\lambda$ (微米) 2		
	1.065	1.061	1.055
	$R(\%)$		
1	0.017	0.015	0.015
2	0.021	0.016	0.010
3	0.024	0.019	0.018
4	0.013	0.015	0.018
5	0.013	0.014	0.013
6	0.020	0.012	0.010
7	0.010	0.010	0.011
8	0.016	0.011	0.010
9	0.010	0.011	0.012
10	0.026	0.018	0.020

Table 11. The results of the low reflectivity measurement of the antireflection films

The authors would like to thank Mr. Wang Muzheng of Jiaotong University for his help in the low reflectivity measurement.

END  
FILMED

5-86

DTIC